

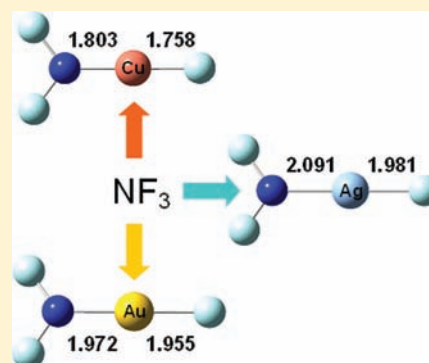
Matrix Infrared Spectroscopic and Theoretical of the Difluoroamino Metal Fluoride Molecules:  $F_2NMF$  ( $M = Cu, Ag, Au$ )

Yu Gong and Lester Andrews\*

Department of Chemistry, University of Virginia, Charlottesville, Virginia 22904-4319, United States

## Supporting Information

**ABSTRACT:** The difluoroamino coinage metal fluoride molecules  $F_2NMF$  ( $M = Cu, Ag, Au$ ) have been made via spontaneous reactions of coinage metals and  $NF_3$  in solid argon and neon matrixes during sample annealing without formation of the  $M(NF_3)$  complexes. Comparisons between the matrix infrared spectra and the density functional frequency calculations provide strong support for identification of the  $F_2NMF$  molecules, which are found to have doublet ground states with  $C_{2v}$  or near  $C_{2v}$  geometries. The  $F_2NCuF$  molecule can isomerize to the less stable  $FNCuF_2$  isomer upon UV–visible irradiation, while no similar reactions were observed for the silver and gold species. The  $M-N$  bonds in the  $F_2NMF$  molecules are stronger than those in the  $FNMF_2$  isomers with the  $Ag-N$  bond being longest and weakest in both cases.



## INTRODUCTION

The catalytic properties of coinage metals ( $Cu, Ag, Au$ ) have been well recognized, as evidenced by a number of reactions catalyzed by compounds with coinage metal centers.<sup>1</sup> Although copper catalysts have been known and used for a long time, reactions mediated by silver and gold catalysts have attracted more attention in recent years.<sup>2</sup> In addition to the rich studies on the applications of coinage metal-involved catalysts, studies on the metal-involved intermediates are also important in understanding the detailed catalytic mechanisms. The amido, imido, and nitrido complexes of coinage metals were considered important intermediates in the formation of new  $C-N$  bonds.<sup>1,3–6</sup> However, the structural information of these transient species is not well established.<sup>7</sup> While progress has been made in synthetic chemistry,<sup>8–11</sup> reactions of metal atoms with nitrogen-containing species can also serve as an effective method to prepare the molecules with direct metal nitrogen bonds. Ammonia is one of the simplest molecules that can be used in these kinds of reactions. Many examples of ammonia and transition metal as well as uranium and thorium reactions have been reported, in which amido and imido metal complexes were produced and characterized via infrared spectroscopy as well as theoretical calculations.<sup>12–16</sup> As a variation,  $NF_3$  is an even better reactant to start with due to the weak  $N-F$  bond, which is only about half as strong as the  $N-H$  bond in ammonia.<sup>17</sup> Recently, a series of experiments on the reactions of transition metals and  $NF_3$  have been carried out in our lab. For uranium and group VI metal atoms, terminal nitride molecules  $NMF_3$  with  $M\equiv N$  triple bonds were characterized, in which the metal centers are in their highest oxidation state of +VI.<sup>18,19</sup> Reactions with group IV and thorium atoms gave rise to terminal pnictinidene  $N\div MF_3$  molecules with two singly occupied  $\pi$  orbitals as the final products, because of the lack

of enough valence electrons to support triple bonds for these tetravalent metal atoms.<sup>20</sup> In addition, fluorine transfer reaction kinetics have also been investigated in the gas phase.<sup>21</sup> In this paper, the reaction products of coinage metals with  $NF_3$  are studied using matrix infrared spectroscopy and density functional calculations, in which the  $F_2NMF$  molecules are identified as the major products. The  $FNCuF_2$  isomer is also produced upon UV–visible irradiation, while no similar products are observed for silver and gold.

## EXPERIMENTAL AND THEORETICAL METHODS

The experimental apparatus and procedure for the preparation of the product molecules in excess argon and neon at 4 K have been described previously.<sup>22</sup> The Nd:YAG laser fundamental (1064 nm, 10 Hz repetition rate with 10 ns pulse width) was focused onto a freshly cleaned copper, silver, or gold target mounted on a rotating rod. Laser-ablated metal atoms were codeposited with 2–4 mmol of argon or neon (Matheson, research) containing 1.0%  $NF_3$  (Air Products) onto a CsI cryogenic window for 60 min (30 min deposition for neon).  $NF_3$  gas was condensed to 77 K using liquid  $N_2$  and evacuated to remove residual  $N_2$  and  $O_2$  before use. FTIR spectra were recorded at 0.5  $cm^{-1}$  resolution on a Nicolet 750 FTIR instrument with a HgCdTe range B detector. Matrix samples were annealed at different temperatures and cooled back to 4 K for spectral acquisition. Selected samples were subjected to broadband photolysis with different glass filters (no filter,  $\lambda > 220$  nm irradiation; Pyrex filter,  $\lambda > 290$  nm irradiation; and yellow glass filter,  $\lambda > 470$  nm irradiation) using a medium-pressure mercury arc street lamp (Philips, 175 W) with the outer globe removed.

Complementary density functional theory (DFT) calculations were performed using the Gaussian 03 program.<sup>23</sup> The hybrid B3LYP density functional was employed in our calculations.<sup>24</sup> The 6-311+G(d) basis set was used for nitrogen, fluorine, and copper

Received: October 6, 2011

Published: December 8, 2011

atoms,<sup>25</sup> and the 28 and 60 electron core SDD pseudopotentials were used for silver and gold.<sup>26</sup> All of the geometrical parameters were fully optimized, and the harmonic vibrational frequencies were obtained analytically at the optimized structures. Transition states for the conversion between  $F_2NMF$  and  $FNMF_2$  isomers were also optimized using the synchronous transit-guided quasi-Newton method implemented in the Gaussian 03 program.

## RESULTS AND DISCUSSION

Experiments with different metals in solid argon revealed that common absorptions due to  $NF_2$  and  $NF$  were produced during sample deposition.<sup>27</sup> Further sample annealing increased  $N_2F_4$  bands, while the  $NF_2$  and  $NF$  absorptions decreased.<sup>28</sup> UV–visible irradiation ( $\lambda > 290$  nm) increased both  $NF$  and  $NF_2$  bands but more for the former, and the  $NF_2$  band decreased slightly when broad band irradiation ( $\lambda > 220$  nm) was used. For comparison, the infrared spectra of an  $NF_3/Ar$  sample deposited at 4 K without metal followed by 30 K annealing and  $\lambda > 220$  nm irradiation are shown in Figure S1, traces h–j (Supporting Information), which produce no  $NF$  and  $NF_2$  absorptions.

**Infrared Spectra.** The infrared spectra from the reactions of copper and  $NF_3$  are shown in Figure 1. Absorptions due to

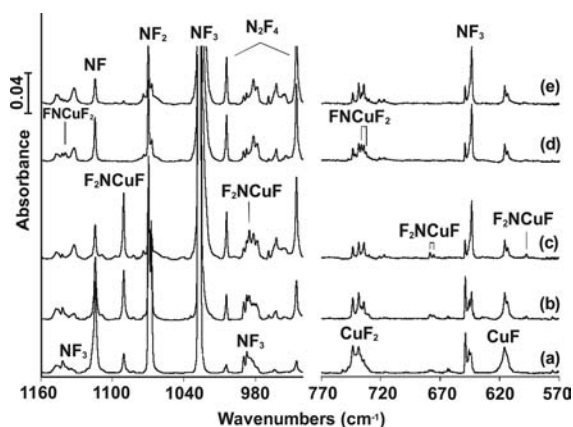


**Figure 1.** Infrared spectra of laser-ablated Cu atom and  $NF_3$  reaction products in solid argon: (a) Cu + 1.0%  $NF_3$  deposition for 60 min, (b) after annealing to 20 K, (c) after annealing to 35 K, (d) after  $\lambda > 290$  nm irradiation, and (e) after annealing to 35 K.

$CuF$  and  $CuF_2$  molecules were observed in the spectrum taken right after sample deposition.<sup>29,30</sup> Additionally, a new metal-dependent band at  $1090.5$   $cm^{-1}$  also appeared (Figure 1, trace a). Subsequent sample annealing results in a substantial growth of this new band. At the same time, another set of absorptions at  $985.0$ ,  $678.4$ ,  $675.5$ , and  $597.5$   $cm^{-1}$  also appeared in the infrared spectra, which have identical behavior with the  $1090.5$   $cm^{-1}$  absorption (Figure 1, traces b and c). UV–visible irradiation with  $\lambda > 290$  nm filter completely destroyed these newly observed absorptions, during which another group of absorptions at  $1139.6$ ,  $736.2$ , and  $732.1$   $cm^{-1}$  increased. These three bands have never been reported previously (Figure 1, trace d). When the sample was annealed again after UV–visible irradiation, the  $1139.6$ ,  $736.2$ , and  $732.1$   $cm^{-1}$  absorptions sharpened first and then decreased slightly, while the  $1090.5$   $cm^{-1}$  band slightly increased (Figure 1, trace e, and Figure S1 in the Supporting Information).

Figure 2 shows the infrared spectra from the reactions of laser-ablated silver atoms with  $NF_3$  in solid argon. Similar with the copper experiment,  $AgF$  and  $AgF_2$  absorptions were the

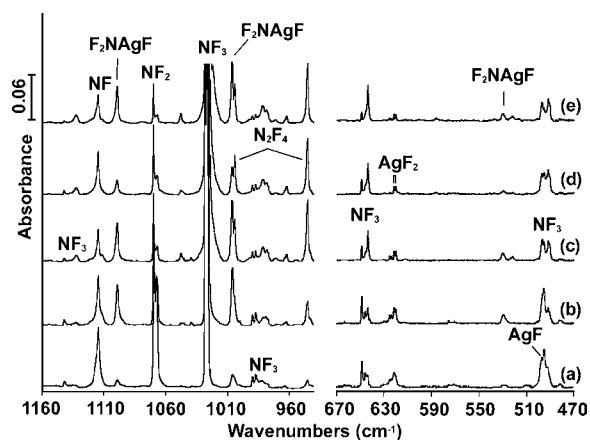


**Figure 2.** Infrared spectra of laser-ablated Ag atom and  $NF_3$  reaction products in solid argon: (a) Ag + 1.0%  $NF_3$  deposition for 60 min, (b) after annealing to 20 K, (c) after annealing to 35 K, (d) after  $\lambda > 220$  nm irradiation, and (e) after annealing to 35 K.

major metal-dependent absorptions right after sample deposition (Figure 2, trace a).<sup>30</sup> New product absorptions at  $1099.2$ ,  $1006.3$ , and  $529.6$   $cm^{-1}$  increased markedly when the sample was annealed to 35 K (Figure 2, trace c). These three absorptions decreased more than half upon broad band irradiation ( $\lambda > 220$  nm) but were produced again during subsequent sample annealing.

Reactions of gold with  $NF_3$  are evidenced by the spectra shown in Figure 3. In addition to the  $(Ar)AuF$  and  $AuF_2$

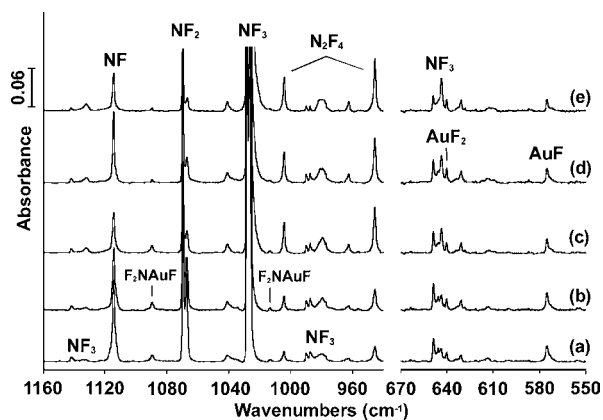


**Figure 3.** Infrared spectra of laser-ablated Au atom and  $NF_3$  reaction products in solid argon: (a) Au + 1.0%  $NF_3$  deposition for 60 min, (b) after annealing to 20 K, (c) after annealing to 35 K, (d) after  $\lambda > 220$  nm irradiation, and (e) after annealing to 35 K.

absorptions observed at  $575.1$  and  $640.1$   $cm^{-1}$ ,<sup>30</sup> two new absorptions at  $1089.7$  and  $1013.4$   $cm^{-1}$  were observed after sample deposition, and they slightly increased during subsequent annealing. Broad band irradiation ( $\lambda > 220$  nm) destroyed these two bands, and they were barely recovered when the sample was annealed further.

The copper, silver, gold, and  $NF_3$  reactions were also repeated in a neon matrix. Common absorptions due to  $NF_2$ ,  $NF$ , and  $NF_3^+$  were observed from the infrared spectra taken after sample deposition.<sup>31</sup> As shown in Figure 4, new metal-dependent absorptions were produced with different coinage metals but with lower yields. All of the new bands were completely destroyed when the samples were subject to UV–

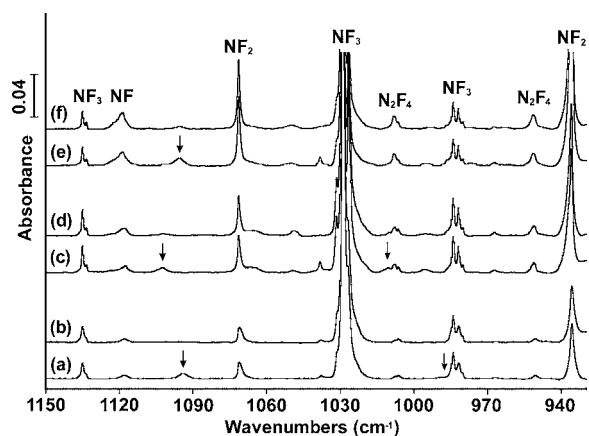


**Figure 4.** Infrared spectra of laser-ablated coinage metal atom and  $\text{NF}_3$  reaction products in solid neon: (a)  $\text{Cu} + 1.0\% \text{NF}_3$  deposition for 30 min followed by annealing to 10 K, (b) after  $\lambda > 290 \text{ nm}$  irradiation, (c)  $\text{Ag} + 1.0\% \text{NF}_3$  deposition for 30 min followed by annealing to 10 K, (d) after  $\lambda > 220 \text{ nm}$  irradiation, (e)  $\text{Au} + 1.0\% \text{NF}_3$  deposition for 30 min followed by annealing to 8 K, and (f) after  $\lambda > 220 \text{ nm}$  irradiation. The arrows indicate the  $\text{F}_2\text{NMF}$  ( $M = \text{coinage metals}$ ) absorptions.

visible irradiation. The product bands observed in argon and neon matrixes are listed in Table 1.

**$\text{F}_2\text{NMF}$  ( $M = \text{Cu, Ag, Au}$ ).** The 1090.5, 985.0, 678.4, 675.5, and 597.5  $\text{cm}^{-1}$  product absorptions have identical behaviors upon sample annealing and irradiation following the copper reaction in excess argon, suggesting that they are due to different vibrational modes of the same molecule (Figure 1). The two strongest absorptions at 1090.5 and 985.0  $\text{cm}^{-1}$  are assigned to N–F stretching modes on the basis of their band positions. Experiments in the neon matrix give two new bands at 1094.3 and 988.2  $\text{cm}^{-1}$ . The neon-to-argon matrix shifts are also near shifts (1–4  $\text{cm}^{-1}$ ) found here for N–F stretching modes in  $\text{NF}_3$ ,  $\text{NF}_2$ , and  $\text{NF}$  (Table 1). In the low frequency region, the relative infrared intensities of the 678.4 and 675.5  $\text{cm}^{-1}$  absorptions are approximately 2:1, which approach the statistical distribution of natural copper isotopes, indicating the involvement of one copper atom in this vibrational mode. The splitting for these two bands is 2.9  $\text{cm}^{-1}$ , slightly larger than that for the diatomic  $\text{CuF}$  molecule (2.2  $\text{cm}^{-1}$ ) observed in the same experiment.<sup>30</sup> Hence, the 678.4 and 675.5  $\text{cm}^{-1}$  absorptions should arise from  $^{63}\text{Cu}$ –F and  $^{65}\text{Cu}$ –F stretching modes coupled with other atoms in such a way that Cu moves antisymmetrically between F and this other atom. Unlike these two bands, the weak band at 597.5  $\text{cm}^{-1}$  shows no splitting of copper isotopes, which means the copper atom is not strongly involved in this mode. Because the bending modes of  $\text{NF}_3$  are also in the same region, the most probable assignment for this weak new band is an  $\text{NF}_2$  bending mode. Accordingly, the newly observed absorptions are assigned to different vibrational modes of the  $\text{F}_2\text{NCuF}$  molecule, which contains the bonds characterized by the above vibrational modes.

In the silver experiment, new product absorptions at 1099.2, 1006.3, and 529.6  $\text{cm}^{-1}$  in solid argon are assigned to the  $\text{F}_2\text{NAgF}$  molecule following the copper example (Figure 2). The first two absorptions should be due to the symmetric and antisymmetric F–N–F stretching modes of the  $\text{NF}_2$  fragment, while the 529.6  $\text{cm}^{-1}$  band arises from the Ag–F stretching mode. Note that the silver isotopic splitting for  $\text{AgF}$  (497.2  $\text{cm}^{-1}$ ) is not resolved, the same as the observed Ag–F mode for

**Table 1.** Observed and Calculated (B3LYP) Vibrational Frequencies for  $\text{NF}_3$  and the  $\text{F}_2\text{NMF}$  and  $\text{FNMF}_2$  Molecules for Coinage Metals (Absorptions above 400  $\text{cm}^{-1}$  Are Listed)

	obsd frequencies		calcd frequencies <sup>a</sup>	assignment
	Ar	Ne		
$\text{NF}_3$	1028.1	1029.3	1034.1 (48)	sym. N–F str.
	898.1	901.3	874.4 (258 × 2)	asym. N–F str.
	648.9	645.1	645.3 (3)	sym. $\text{NF}_3$ deform.
	494.9	492.4	484.9 (2 × 2)	asym. $\text{NF}_3$ deform.
$\text{F}_2\text{NCuF}$	1090.5	1094.3	1117.4 (369)	sym. F–N–F str.
	985.0	988.2	971.9 (187)	asym. F–N–F str.
	678.4	<i>b</i>	664.1 (83)	$^{63}\text{Cu}$ –F str. <sup>c</sup>
	597.5	<i>b</i>	588.9 (11)	$\text{NF}_2$ bend.
$\text{F}_2\text{NAgF}$	1099.2	1102.4	1083.1 (421)	sym. F–N–F str.
	1006.3	1010.8	979.2 (207)	asym. F–N–F str.
	<i>b</i>	<i>b</i>	591.2 (1)	$\text{NF}_2$ bend.
	529.6	<i>b</i>	531.0 (72)	Ag–F str.
$\text{F}_2\text{NAuF}$	1089.7	1095.3	1077.4 (416)	sym. F–N–F str.
	1013.4	<i>b</i>	982.9 (185)	asym. F–N–F str.
	<i>b</i>	<i>b</i>	605.1 (8)	$\text{NF}_2$ bend.
	<i>b</i>	<i>b</i>	572.7 (73)	Au–F str.
$\text{FNCuF}_2$	1139.6	<i>b</i>	1189.0 (267)	N–F str.
	736.2	<i>b</i>	707.7 (136)	asym. F– $^{63}\text{Cu}$ –F str. <sup>d</sup>
$\text{FNAgF}_2$ <sup>e</sup>	<i>b</i>	<i>b</i>	564.2 (10)	sym. F– $^{63}\text{Cu}$ –F str.
			1157.5 (340)	N–F str.
			610.3 (111)	asym. F–Ag–F str.
			509.0 (8)	sym. F–Ag–F str.
$\text{FNAuF}_2$ <sup>e</sup>			1096.8 (337)	N–F str.
			605.4 (122)	asym. F–Au–F str.
			559.2 (18)	sym. F–Au–F str.
			541.5 (14)	Au–NF str.

<sup>a</sup>Frequencies in  $\text{cm}^{-1}$  and intensities (in parentheses) in  $\text{km/mol}$ . <sup>b</sup>Not observed. <sup>c</sup> $^{65}\text{Cu}$ –F str. observed at 675.5  $\text{cm}^{-1}$  and calculated at 661.1  $\text{cm}^{-1}$ . <sup>d</sup>Asym. F– $^{65}\text{Cu}$ –F str. observed at 732.1  $\text{cm}^{-1}$  and calculated at 703.6  $\text{cm}^{-1}$ . <sup>e</sup>Not formed.

$\text{F}_2\text{NAgF}$ . The two N–F modes of the  $\text{F}_2\text{NAgF}$  molecule in solid neon are slightly blue-shifted from their argon counterparts, similar with the case of the copper analog (Figure 4).

Two weak absorptions at 1089.7 and 1013.4  $\text{cm}^{-1}$  were observed in the reactions of Au and  $\text{NF}_3$  in solid argon (Figure 3). They are most probably due to the symmetric and antisymmetric F–N–F stretching modes of the  $\text{F}_2\text{NAuF}$  molecule, respectively, based on the band positions as well as the small matrix shifts from neon to argon.

The assignments of the  $\text{F}_2\text{NMF}$  ( $M = \text{Cu, Ag, Au}$ ) molecules are supported by density functional calculations at the B3LYP level of theory. For the  $\text{F}_2\text{NCuF}$  product, the  ${}^2\text{B}_1$  state with planar  $\text{C}_{2v}$  symmetry is found to be the ground state (Figure 5). Four infrared absorptions at 1117.4, 971.9, 664.1, and 588.9  $\text{cm}^{-1}$  are predicted above 400  $\text{cm}^{-1}$  from frequency calculations. The first two bands are due to symmetric and antisymmetric F–N–F stretching modes of the  $\text{NF}_2$  fragment with the former being twice as strong as the latter one. The positions of these two bands are slightly higher and lower than the observed frequencies, which is similar to our results for  $\text{NF}_3$  (Table 1) and in the range of agreement found for other simple molecules.<sup>32</sup> The Cu–F stretching mode is predicted at 664.1  $\text{cm}^{-1}$  with a copper isotopic splitting of 3.0  $\text{cm}^{-1}$ , almost the same as the experimental value. For the  $\text{NF}_2$  bending mode, the

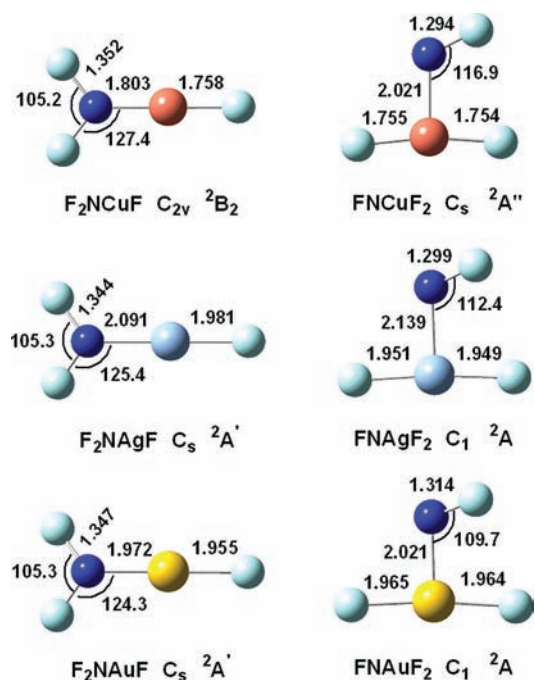


**Figure 5.** Structures of the F<sub>2</sub>NMF and FNMF<sub>2</sub> (M = coinage metals) molecules calculated at the DFT/B3LYP level of theory (bond lengths are in Angstrom units, and bond angles are in degrees).

calculated 588.9 cm<sup>-1</sup> band is also close to the experimental frequency at 597.5 cm<sup>-1</sup>.

The F<sub>2</sub>NAgF molecule also possesses a doublet ground state with slightly distorted C<sub>2v</sub> symmetry, as evidence by the sum of two Ag–N–F and one F–N–F angle (356.1°) (Figure 5). Similar with the copper product, our calculations reveal that the F<sub>2</sub>NAgF molecule has four absorptions at 1083.1, 979.2, 591.2, and 531.0 cm<sup>-1</sup> above 400 cm<sup>-1</sup>. However, the 591.2 cm<sup>-1</sup> band due to the NF<sub>2</sub> bending mode is too weak (Table 1), which results in its absence in the experiment. The calculated 1083.1 and 979.2 cm<sup>-1</sup> absorptions are slightly lower than the experimentally observed symmetric and antisymmetric F–N–F stretching modes. Calculations on the silver isotopes reveal that the Ag–F stretching mode for the F<sub>2</sub>N<sup>107</sup>AgF and F<sub>2</sub>N<sup>109</sup>AgF molecules are only separated by 0.8 cm<sup>-1</sup>, which is too small to be resolved experimentally. As a result, only a single band is observed for this mode. The F<sub>2</sub>NAuF molecule is calculated to have very strong absorptions at 1077.4 and 982.9 cm<sup>-1</sup> with relative intensities of approximately 2:1, which fit the experimental frequencies at 1089.7 and 1013.4 cm<sup>-1</sup>. While the weaker absorptions of NF<sub>2</sub> bending and Au–F stretching modes are predicted at 605.1 and 572.7 cm<sup>-1</sup>, they were not observed due to the low yield of the F<sub>2</sub>NAuF molecule.

As shown in Figure 5, the M–F bond lengths (M = coinage metals) increase from copper to silver but slightly decrease for gold, which is also the trend observed for the coinage metal fluoride molecules.<sup>30</sup> The shorter bond lengths for the gold-containing molecules result from the relativistic effects of gold.<sup>33</sup> A similar trend is observed for the calculated M–N distances. The Ag–N bond length is calculated to be 2.091, 0.119, and 0.288 Å longer than those of gold and copper. To compare further the M–N bond strengths of different coinage metals, the dissociation energies of the F<sub>2</sub>N–MF bonds are calculated at the B3LYP level of theory. It is found that the Cu–N (27.5 kcal/mol) and Au–N (26.5 kcal/mol) bonds are

stronger than that of silver (12.2 kcal/mol), which is also in line with changes in the M–N bond lengths. Recent gas phase studies on the dimethylaminonitrene complexes of coinage metals revealed that the M–N bond strengths for copper and gold are similar but about 5 kcal/mol higher than that of silver.<sup>34</sup> This is consistent with the fact that silver has the longest bond length followed by gold and copper. It appears that this kind of change in bond lengths and strengths is common for coinage metals, which is also the case for the M–C bonds in the CH<sub>3</sub>MH and CH<sub>3</sub>MF molecules produced from the reactions of coinage metals with CH<sub>4</sub> and CH<sub>3</sub>F.<sup>35,36</sup>

The molecular orbitals of the F<sub>2</sub>NMF molecules reveal that the unpaired electron is delocalized over the whole molecule, which contains some M–N π\* character in addition to the doubly occupied π orbital. Hence, beyond the M–N σ bond, the M–N bond also exhibits weak π interactions due to its singly occupied nature. Actually, the Cu–N distance (1.803 Å) is slightly lower than the sum of copper and nitrogen single bond radii,<sup>37</sup> suggesting that the Cu–N bond in the F<sub>2</sub>NCuF molecule is slightly more than a single bond. Recent theoretical and experimental studies on the copper nitrene species also gave similar Cu–N bond distances, which are expected to have some Cu–N double bond character.<sup>6,9</sup> For the F<sub>2</sub>NAuF molecule, the calculated Au–N bond length of 1.972 Å is about 0.04 Å shorter than the value in the amido gold complex.<sup>10</sup> The recently identified CH<sub>2</sub>AuF molecule was proposed to have a Au=C double bond with some π character.<sup>35</sup> Spin density calculations for all three molecules predict that most of the electron spin density is on nitrogen atom (more than 65%), which contributes to the weak π interactions.

**FNCuF<sub>2</sub>.** Three absorptions at 1139.6, 736.2, and 732.1 cm<sup>-1</sup> were produced upon λ > 290 nm irradiation, during which the F<sub>2</sub>NCuF absorptions disappeared. Hence, these new bands could arise from a structural isomer of the F<sub>2</sub>NCuF molecule. The 736.2 and 732.1 cm<sup>-1</sup> absorptions are about 7 cm<sup>-1</sup> red-shifted from the isolated CuF<sub>2</sub> band, and the 4.1 cm<sup>-1</sup> split is almost the same as that of CuF<sub>2</sub> (4.2 cm<sup>-1</sup>) observed in the same experiment. As a result, these two bands are assigned to the antisymmetric F–<sup>63</sup>Cu–F and F–<sup>65</sup>Cu–F stretching modes of the new molecule. The 1139.6 cm<sup>-1</sup> band should be an N–F stretching vibrational mode on the basis of the band position. Hence, a FNCuF<sub>2</sub> complex with NF and CuF<sub>2</sub> subgroups is proposed as the most probable origin of the new absorptions. Earlier matrix infrared spectra of the CuF<sub>2</sub> molecule produced from evaporation of bulk material revealed two weak matrix site bands of CuF<sub>2</sub> at 736.5 and 732.6 cm<sup>-1</sup>,<sup>38</sup> which were not observed in our recent experiments on the reactions of laser-ablated copper atoms and F<sub>2</sub>.<sup>30</sup> It is obvious that the appearance of the 1139.6 cm<sup>-1</sup> absorption together with the 736.2 and 732.1 cm<sup>-1</sup> bands provides adequate evidence for the assignment of the FNCuF<sub>2</sub> complex in our current experiments.

Calculations at B3LYP level of theory reveal that the FNCuF<sub>2</sub> molecule has a planar geometry and doublet ground state (Figure 5). The N–F stretching mode is predicted at 1189.0 cm<sup>-1</sup>, which is also the strongest band of the product. For the CuF<sub>2</sub> moiety, the antisymmetric and symmetric F–Cu–F modes are calculated at 707.7 and 564.2 cm<sup>-1</sup> with the relative intensities of 13:1 (Table 1). Experimentally, the product absorptions are observed at 1139.6 and 736.2 cm<sup>-1</sup>, while the symmetric F–Cu–F mode is too weak to be observed here. In addition, the splitting for the antisymmetric F–Cu–F

stretching mode due to copper isotopes is calculated to be 4.1  $\text{cm}^{-1}$ , the same as the experimental value. The Cu–N distance is predicted to be 2.021 Å, about 0.2 Å longer than that in the  $\text{F}_2\text{NCuF}$  molecule as well as the bond length proposed for single Cu–N bond.<sup>37</sup> The calculated dissociation energy of the FN–CuF<sub>2</sub> bond is 11.9 kcal/mol [relative to CuF<sub>2</sub> and (<sup>3</sup>Σ) NF], less than half of the value for the Cu–N bond in the  $\text{F}_2\text{NCuF}$  molecule, suggesting that CuF<sub>2</sub> and NF are weakly bound in the FNCuF<sub>2</sub> molecule. This is also consistent with the longer computed Cu–N bond length in the FNCuF<sub>2</sub> molecule. Although a nitrene complex might be expected in this case due to the availability of two electrons on nitrogen, the formation of a Cu=N double bond would require a copper(IV) center, which is an uncommon oxidation state for copper.<sup>39</sup> We find no evidence for CuF<sub>4</sub> in ongoing fluorine work in this laboratory,<sup>30</sup> despite the fact that the neutral CuF<sub>4</sub> molecule was predicted to be stable.<sup>40</sup> In summary, the FNCuF<sub>2</sub> molecule contains a long computed Cu–N bond length with a Cu(II)-like metal center.

In addition to the observed FNCuF<sub>2</sub> molecule, calculations using the B3LYP functional are also performed on the unobserved silver and gold analogs. As shown in Figure 5, the optimized structures of the FNAgF<sub>2</sub> and FNAuF<sub>2</sub> molecules are quite similar. Both of them have doublet ground states with the N–F moiety slightly out of the F<sub>2</sub>AgN and F<sub>2</sub>AuN plane. The Ag–N and Au–N bond distances are only slightly longer (about 0.05 Å) than those in the F<sub>2</sub>NAgF and F<sub>2</sub>NAuF molecules with the Ag–N and Au–N bond energies calculated to be 10.1 and 19.0 kcal/mol, suggesting that the metal nitrogen bonds are also weakened upon the second fluorine transfer but not as much as that for copper. Frequency calculations reveal that both of them have strong N–F stretching absorptions around 1100  $\text{cm}^{-1}$  followed by strong metal–fluorine stretches around 600  $\text{cm}^{-1}$  (Table 1).

**Reactions in the Matrix.** As shown in Figures 1–3, the F<sub>2</sub>NMF (M = coinage metal) molecules are produced spontaneously via the reactions of coinage metals with NF<sub>3</sub> upon sample annealing. This is in contrast to the copper reaction with ammonia, which required irradiation for insertion into the N–H bond.<sup>13</sup> No M(NF<sub>3</sub>) complexes were observed in the experiments. Our geometry optimizations on the different structures of molecular complexes give rather long N–M or F–M distances. Hence, the M(NF<sub>3</sub>) complexes are not stable minima along the reaction coordinates of coinage metals and NF<sub>3</sub>. The spontaneous productions of the F<sub>2</sub>NMF molecules indicate that negligible activation energies are required for one fluorine transfer from NF<sub>3</sub> to the coinage metals. Reactions (1) for coinage metals are predicted to be exothermic with copper being the highest followed by gold and silver (Table 2). Note that all of the coinage metals in the

gold(II) centers are not as common as the gold(I) and (III) species due to the tendency of disproportionation for Au(II) to the other two oxidation states.<sup>42</sup> Our recent studies revealed that divalent gold species can be prepared via insertion into the single bond of some simple molecules.<sup>35,36,43,44</sup>



Different from the NF<sub>3</sub> reactions reported here, thermally evaporated copper atoms reacted with ammonia in solid argon to give the Cu(NH<sub>3</sub>) complex first, which isomerized to HCuNH<sub>2</sub> upon UV irradiation via N–H bond insertion.<sup>13</sup> The Cu(NH<sub>3</sub>) complex was characterized to have a direct Cu–N interaction from theoretical calculations.<sup>45</sup> However, no similar Cu(NF<sub>3</sub>) complex was observed in the reactions of Cu and NF<sub>3</sub>, which is also supported by the spontaneous formation of the F<sub>2</sub>NCuF molecule on annealing. The weak N–F bond makes the insertion reaction easier than that for N–H bond,<sup>17</sup> which probably accounts for the spontaneous formation of the F<sub>2</sub>NCuF molecule. Because fluorine is the most electronegative atom, the lone pair electronic density of NF<sub>3</sub> is reduced, and the dipole moment direction is also reversed as compared with those of NH<sub>3</sub>,<sup>46</sup> both of which make it less favorable to form the Cu(NF<sub>3</sub>) complex with a Cu–N interaction. This is also consistent with our results on the geometry optimizations of the Cu(NF<sub>3</sub>) system. Note that NF<sub>3</sub> is a very weak base and can only form a weakly bonded complex with BF<sub>3</sub> (B–N dissociation energy, 1.8 kcal/mol), and BF<sub>3</sub> is known as a strong Lewis acid. In contrast, the binding energy of the F<sub>3</sub>B–NH<sub>3</sub> adduct is more than 20 kcal/mol.<sup>47</sup>

In the reactions of copper and NF<sub>3</sub>, the FNCuF<sub>2</sub> isomer is identified on the basis of the N–F and F–Cu–F stretching modes. However, no trace can be found for the formation of similar products in the silver and gold reactions under the same conditions, suggesting that it is not favorable to form the analogous molecules with heavier coinage metals. Calculations on the isomerization pathways between F<sub>2</sub>NMF and FNMF<sub>2</sub> isomers reveal that the formation of the FNCuF<sub>2</sub> molecule is prohibited by an energy barrier of 18.0 kcal/mol, while the activation energies for silver and gold are calculated to be 30.9 and 33.2 kcal/mol (Table 2). Because the barrier heights for producing FNAgF<sub>2</sub> and FNAuF<sub>2</sub> molecules are about twice as high as that for copper, formations of these heavier analogs are not favored because of kinetic reasons. Although the UV photon energies used are higher than the energy barriers for all of the metals, the successful formation of the isomerization products also requires access to the corresponding excited electronic states of FNAgF<sub>2</sub> and FNAuF<sub>2</sub>, which probably do not happen with the radiation employed. These excited states are not calculated theoretically here. In addition, our calculations also indicate that formation of the FNCuF<sub>2</sub> molecule is more favorable thermodynamically. The FNCuF<sub>2</sub> molecule is predicted to be only 4.5 kcal/mol less stable than the F<sub>2</sub>NCuF isomer, while the values for silver and gold are 20.0 and 14.6 kcal/mol, respectively. After FNCuF<sub>2</sub> was produced by  $\lambda > 290$  nm irradiation, annealing to 30 K sharpened these absorptions, but annealing to 35 K slightly decreased these bands (Figure S1 in the Supporting Information). Annealing to such “high” temperature as 35 K in solid argon allows diffusion and aggregation of isolated species, and these aggregates have broader absorptions than the previously isolated species, which is common in matrix infrared spectroscopy.<sup>22</sup>

**Table 2. Computed (B3LYP) Energies (Relative to Ground State Coinage Metal Atoms and NF<sub>3</sub>, kcal/mol) of the F<sub>2</sub>NMF and FNMF<sub>2</sub> Molecules as Well as the Transition States**

	F <sub>2</sub> NMF	TS	FNMF <sub>2</sub>
Cu	−68.3	−50.3	−63.8
Ag	−35.4	−4.5	−15.4
Au	−37.1	−3.9	−22.5

F<sub>2</sub>NMF molecules are in the II oxidation state. Although this is common for species with copper and divalent silver fluorides and oxides are also available,<sup>30,41</sup> molecules with a mononuclear

The  $F_2NMF$  molecules were all photosensitive:  $F_2NCuF$  was completely destroyed by  $\lambda > 290$  nm irradiation, and the  $FNCuF_2$  isomer as well as  $NF$  and  $NF_2$  species were produced. In the Ag and Au experiments,  $\lambda > 290$  nm irradiation initiated the formation of  $NF$  and  $NF_2$ , and  $\lambda > 220$  nm irradiation slightly continued the growth of  $NF$ , while both  $F_2NAgF$  and  $F_2NAuF$  absorptions decreased. Figure S1 (Supporting Information) shows expanded scale spectra in the important 1160–1060 and 760–720  $cm^{-1}$  regions containing all of the experimental changes from the Cu and  $NF_3$  reactions ( $^{63}Cu$  and  $^{65}Cu$  isotopes observed for  $CuF_2$  and  $FNCuF_2$  are indicated). Because  $NF$  and  $NF_2$  were not observed in the blank experiment without metal atoms, decomposition of the  $F_2NMF$  molecules to  $NF$  and  $NF_2$  species should be considered. Also, we could not rule out nor detect any reformation of coinage metals and  $NF_3$  because metal atoms do not have absorptions in the midinfrared region, while the  $NF_3$  precursor bands are huge and their band shapes change upon sample annealing and irradiation. Although reactions of metal atoms with  $NF$  and  $NF_2$  are possible, the weaker intensities of these species as compared with  $NF_3$  makes it unlikely for them to form enough molecules to be detected by matrix infrared spectroscopy.

The recently reported  $N\equiv MF_3$  ( $M$  = group VI and uranium) molecules were characterized to have triple metal–nitrogen bonds,<sup>18,19</sup> while the pnictinidene  $N\div MF_3$  molecules with two radical  $\pi$  bonds were produced for group IV and thorium atoms.<sup>20</sup> All of these species are found to be most stable among the products from stepwise fluorine transfer reactions. However, reactions of coinage metals and  $NF_3$  give the  $F_2NMF$  molecules as the most stable products. The two fluorine transfer molecules are higher in energy, which is apparently the result of the weak  $FN-MF_2$  bonds since both the  $N-F$  and the coinage metal– $F$  bond strengths are comparable.<sup>48,49</sup> For uranium and group VI metals, the  $M-N$  bond orders increase with the stepwise transfer of fluorine from nitrogen to metal center, which is expected to be energetically favorable.<sup>18,19</sup> The VI oxidation state also makes it possible for the formation of triply bonded species. The pnictinidene  $N\div MF_3$  molecules satisfies the IV oxidation state of group IV and thorium atoms, and formation of the strong  $M-F$  bonds provides the driving force for the fluorine transfer from nitrogen to metal.<sup>20</sup>

The spectra from the reactions of coinage metals with  $NF_3$  also show some other features in addition to the product bands mentioned above. New absorptions on the lower sides of the  $CuF_2$  and  $AuF_2$  bands and higher side of the  $AgF_2$  band were produced in different experiments. The 738.4 and 734.0  $cm^{-1}$  absorptions observed in the copper experiment show a similar splitting with  $CuF_2$  due to copper isotopes, suggesting that a new complex of  $CuF_2$  is formed here (Figure S1 in the Supporting Information). The most probable assignment for the new species is the  $(NF_3)CuF_2$  complex since the amount of  $NF_3$  is much more than other molecules in the same matrix sample. Similar tentative assignments can be made to the doublet band (625.4 and 623.9  $cm^{-1}$ ) produced in the silver experiments and the single band observed at 630.7  $cm^{-1}$  for gold. Our B3LYP calculations predict that all of the  $(NF_3)MF_2$  complexes ( $M$  = coinage metal) with some metal nitrogen interactions are stable. In the  $N-F$  stretching region, some weak metal-dependent absorptions were observed as well, which probably track the lower fluoride stretching modes and

arise from the  $N-F$  stretching vibrations of the  $(NF_3)MF_2$  complexes.

## CONCLUSIONS

The reactions of coinage metals (Cu, Ag, Au) with  $NF_3$  have been studied in argon and neon matrixes. Reaction products are characterized by infrared spectroscopy and density functional calculations. Ground state coinage metal atoms react with  $NF_3$  spontaneously to give the amido  $F_2NMF$  molecules via insertion into the weak  $N-F$  bond during sample annealing. All three products are predicted to have doublet ground states with  $C_{2v}$  or near  $C_{2v}$  geometries. Both the bond lengths and the energies suggest strong  $M-N$  interactions, which are believed to be slightly more than single bonds. The  $Ag-N$  bond is found to be longer and weaker than that of the other two coinage metals. No trace can be found for the formation of the  $M(NF_3)$  complexes, which are also predicted to be unstable along the reaction coordinates of coinage metals and  $NF_3$ . UV–visible irradiation induces formation of the less stable  $FNCuF_2$  isomer with a weaker  $Cu-N$  bond, while the silver and gold analogs are not observed, the formation of which are both kinetically and thermodynamically less favorable than that of  $FNCuF_2$ . Our calculations suggest that the  $M-N$  bonds of the  $FNMF_2$  isomers are weaker and longer than those of the  $F_2NMF$  molecules.

## ASSOCIATED CONTENT

### Supporting Information

Figure S1 of expanded scale infrared spectra from an experiment using Cu and  $NF_3$  and from a blank experiment with argon/ $NF_3$  and no metal atoms. This material is available free of charge via the Internet at <http://pubs.acs.org>.

## AUTHOR INFORMATION

### Corresponding Author

\*E-mail: [lsa@virginia.edu](mailto:lsa@virginia.edu).

## ACKNOWLEDGMENTS

We gratefully acknowledge financial support from DOE Grant No. DE-SC0001034.

## REFERENCES

- (1) Díaz-Requejo, M. M.; Pérez, P. J. *Chem. Rev.* **2008**, *108*, 3379–3394.
- (2) Lipshutz, B. H.; Yamamoto, Y. *Chem. Rev.* **2008**, *108*, 2793–2795.
- (3) (a) Li, Z.; Quan, R. W.; Jacobsen, E. N. *J. Am. Chem. Soc.* **1995**, *117*, 5889–5890. (b) Díaz-Requejo, M. M.; Pérez, P. J.; Brookhart, M.; Templeton, J. L. *Organometallics* **1997**, *16*, 4399–4402. (c) Gillespie, K. M.; Crust, E. J.; Deeth, R. J.; Scott, P. *Chem. Commun.* **2001**, 785–786.
- (4) (a) Li, Z. G.; He, C. *Eur. J. Org. Chem.* **2006**, 4313–4322. (b) Gómez-Emeterio, B. P.; Urbano, J.; Díaz-Requejo, M. M.; Pérez, P. J. *Organometallics* **2008**, *27*, 4126–4130.
- (5) Brandt, P.; Södergren, M. J.; Andersson, P. G.; Norrby, P. O. *J. Am. Chem. Soc.* **2000**, *122*, 8013–8020.
- (6) (a) Cundari, T. R.; Dinescu, A.; Kazi, A. B. *Inorg. Chem.* **2008**, *47*, 10067–10072. (b) Meng, Q.; Wang, F.; Qu, X.; Zhou, J.; Li, M. *THEOCHEM* **2007**, *815*, 111–118.
- (7) Berry, J. F. *Comments Inorg. Chem.* **2009**, *30*, 28–66.
- (8) Mohamed, A. A. *Coord. Chem. Rev.* **2010**, *254*, 1918–1947.
- (9) Badiei, Y. M.; Krishnaswamy, A.; Melzer, M. M.; Warren, T. H. *J. Am. Chem. Soc.* **2006**, *128*, 15056–15057.

- (10) Cinelli, M. A.; Minghetti, G.; Pinna, M. V.; Stoccoro, S.; Zucca, A.; Manassero, M. *Eur. J. Inorg. Chem.* **2003**, 2304–2310.
- (11) Martín, A.; Martínez-Espada, N.; Mena, M.; Yélamos, C. *Chem. Commun.* **2007**, 2983–2985.
- (12) (a) Chen, M. H.; Lu, H.; Dong, J.; Miao, L.; Zhou, M. F. *J. Phys. Chem. A* **2002**, *106*, 11456–11464. (b) Zhou, M. F.; Chen, M. H.; Zhang, L. N.; Lu, H. *J. Phys. Chem. A* **2002**, *106*, 9017–9023.
- (13) Ball, D. W.; Hauge, R. H.; Margrave, J. L. *Inorg. Chem.* **1989**, *28*, 1599–1601.
- (14) (a) Kauffman, J. W.; Hauge, R. H.; Margrave, J. L. *High Temp. Sci.* **1984**, *17*, 237–249. (b) Ball, D. W.; Hauge, R. H.; Margrave, J. L. *High Temp. Sci.* **1988**, *25*, 95–101.
- (15) (a) Wang, X. F.; Andrews, L.; Marsden, C. J. *Chem.—Eur. J.* **2008**, *14*, 9192–9201. (b) Wang, X. F.; Andrews, L.; Marsden, C. J. *Chem.—Eur. J.* **2007**, *13*, 5601–5606.
- (16) Wang, X. F.; Andrews, L. *Organometallics* **2008**, *27*, 4885–4891.
- (17) (a) Berkowitz, J.; Greene, J. P.; Foropoulos, J.; Nesković, O. M. *J. Chem. Phys.* **1984**, *81*, 6166–6175. (b) Gibson, S. T.; Greene, J. P.; Berkowitz, J. *J. Chem. Phys.* **1985**, *83*, 4319–4328.
- (18) Wang, X. F.; Andrews, L.; Lindh, R.; Veryazov, V.; Roos, B. O. *J. Phys. Chem. A* **2008**, *112*, 8030–8037.
- (19) Andrews, L.; Wang, X. F.; Lindh, R.; Roos, B. O.; Marsden, C. J. *Angew. Chem., Int. Ed.* **2008**, *47*, 5366–5370.
- (20) (a) Wang, X. F.; Lyon, J. T.; Andrews, L. *Inorg. Chem.* **2009**, *48*, 6297–6302. (b) Wang, X. F.; Andrews, L. *Dalton Trans.* **2009**, 9260–9265.
- (21) Zhao, X.; Koyanagi, G. K.; Bohme, D. K. *J. Phys. Chem. A* **2006**, *110*, 10607–10618.
- (22) (a) Andrews, L.; Citra, A. *Chem. Rev.* **2002**, *102*, 885–911. (b) Andrews, L. *Chem. Soc. Rev.* **2004**, *33*, 123–132. (c) Andrews, L.; Cho, H.-G. *Organometallics* **2006**, *25*, 4040–4053, and references therein.
- (23) Frisch, M. J.; Trucks, G. W.; Schlegel, H. B.; Scuseria, G. E.; Robb, M. A.; Cheeseman, J. R.; Montgomery, J. A., Jr.; Vreven, T.; Kudin, K. N.; Burant, J. C.; Millam, J. M.; Iyengar, S. S.; Tomasi, J.; Barone, V.; Mennucci, B.; Cossi, M.; Scalmani, G.; Rega, N.; Petersson, G. A.; Nakatsuji, H.; Hada, M.; Ehara, M.; Toyota, K.; Fukuda, R.; Hasegawa, J.; Ishida, M.; Nakajima, T.; Honda, Y.; Kitao, O.; Nakai, H.; Klene, M.; Li, X.; Knox, J. E.; Hratchian, H. P.; Cross, J. B.; Bakken, V.; Adamo, C.; Jaramillo, J.; Gomperts, R.; Stratmann, R. E.; Yazyev, O.; Austin, A. J.; Cammi, R.; Pomelli, C.; Ochterski, J. W.; Ayala, P. Y.; Morokuma, K.; Voth, G. A.; Salvador, P.; Dannenberg, J. J.; Zakrzewski, V. G.; Dapprich, S.; Daniels, A. D.; Strain, M. C.; Farkas, O.; Malick, D. K.; Rabuck, A. D.; Raghavachari, K.; Foresman, J. B.; Ortiz, J. V.; Cui, Q.; Baboul, A. G.; Clifford, S.; Cioslowski, J.; Stefanov, B. B.; Liu, G.; Liashenko, A.; Piskorz, P.; Komaromi, I.; Martin, R. L.; Fox, D. J.; Keith, T.; Al-Laham, M. A.; Peng, C. Y.; Nanayakkara, A.; Challacombe, M.; Gill, P. M. W.; Johnson, B.; Chen, W.; Wong, M. W.; Gonzalez, C.; Pople, J. A. *Gaussian 03*, revision E.01; Gaussian, Inc.: Wallingford, CT, 2003.
- (24) (a) Becke, A. D. *J. Chem. Phys.* **1993**, *98*, 5648–5652. (b) Lee, C.; Yang, W.; Parr, R. G. *Phys. Rev. B* **1988**, *37*, 785–789.
- (25) (a) McLean, A. D.; Chandler, G. S. *J. Chem. Phys.* **1980**, *72*, 5639–5648. (b) Krishnan, R.; Binkley, J. S.; Seeger, R.; Pople, J. A. *J. Chem. Phys.* **1980**, *72*, 650–654. (c) Wachters, A. J. H. *J. Chem. Phys.* **1970**, *52*, 1033–1036. (d) Hay, P. J. *J. Chem. Phys.* **1977**, *66*, 4377–4384.
- (26) (a) Andrae, D.; Haussermann, U.; Dolg, M.; Stoll, H.; Preuss, H. *Theor. Chim. Acta* **1990**, *77*, 123–141. (b) Dolg, M.; Stoll, H.; Preuss, H. *J. Chem. Phys.* **1989**, *90*, 1730–1734.
- (27) Jacox, M. E.; Milligan, D. E. *J. Chem. Phys.* **1967**, *46*, 184–191.
- (28) Shchepkin, D. N.; Zhygula, L. A.; Belozerskaya, L. P. *J. Mol. Struct.* **1978**, *49*, 266–273.
- (29) Hastie, J. W.; Hauge, R.; Margrave, J. L. *High Temp. Sci.* **1969**, *1*, 76–85.
- (30) Wang, X. F.; Riedel, S.; Andrews, L. Unpublished frequencies of coinage metal fluorides measured in an argon matrix ( $\text{cm}^{-1}$ ):  $^{63}\text{CuF}$  (615.9),  $^{65}\text{CuF}$  (613.7),  $\text{AgF}$  (497.2),  $\text{AuF}$  (575.1),  $^{63}\text{CuF}_2$  (743.5),  $^{65}\text{CuF}_2$  (738.9),  $^{107}\text{AgF}_2$  (621.5),  $^{109}\text{AgF}_2$  (620.2), and  $\text{AuF}_2$  (640.1).
- (31) Jacox, M. E.; Thompson, W. E. *J. Chem. Phys.* **1995**, *102*, 6–12.
- (32) (a) Andersson, M. P.; Uvdal, P. L. *J. Phys. Chem. A* **2005**, *109*, 2937–2941. (b) Merrick, J. P.; Moran, D.; Radom, L. *J. Phys. Chem. A* **2007**, *111*, 11683–11700. (c) Chertihin, G. V.; Andrews, L.; Bauschlicher, C. W. Jr. *J. Phys. Chem. A* **1997**, *101*, 4026–4034.
- (33) Pyykkö, P. *Angew. Chem., Int. Ed.* **2004**, *43*, 4412–4456.
- (34) Fedorov, A.; Couzijn, E. P. A.; Nagornova, N. S.; Boyarkina, O. V.; Rizzo, T. R.; Chen, P. *J. Am. Chem. Soc.* **2010**, *132*, 13789–13798.
- (35) Cho, H. G.; Andrews, L. *Inorg. Chem.* **2011**, *50*, 10319–10327.
- (36) Cho, H. G.; Andrews, L. *Dalton Trans.* **2011**, *40*, 11115–11124.
- (37) Pyykkö, P.; Atsumi, M. *Chem.—Eur. J.* **2009**, *15*, 186–197.
- (38) Van Leirsburg, D. A.; DeKock, C. W. *J. Phys. Chem.* **1974**, *78*, 134–142.
- (39) Riedel, S.; Kaupp, M. *Coord. Chem. Rev.* **2009**, *253*, 606–624.
- (40) (a) Wang, Q.; Sun, Q.; Jena, P. *J. Chem. Phys.* **2009**, *131*, 124301. (b) Koirala, P.; Willis, M.; Kiran, B.; Kandalam, A. K.; Jena, P. *J. Phys. Chem. C* **2010**, *114*, 16018–16024.
- (41) Cotton, F. A.; Wilkinson, G.; Murillo, C. A.; Bochmann, M. *Advanced Inorganic Chemistry*, 6th ed.; Wiley: New York, 1999.
- (42) Laguna, A.; Laguna, M. *Coord. Chem. Rev.* **1999**, *193–195*, 837–856.
- (43) Wang, X. F.; Andrews, L. *Inorg. Chem.* **2005**, *44*, 9076–9083.
- (44) Wang, X. F.; Andrews, L. *Chem. Commun.* **2005**, 4001–4003.
- (45) Pápai, I. *J. Chem. Phys.* **1995**, *103*, 1860–1870.
- (46) Blanco, F.; Alkorta, I.; Rozas, I.; Solimannejad, M.; Elguero, J. *Phys. Chem. Chem. Phys.* **2011**, *13*, 674–683.
- (47) Antoniotti, P.; Borocci, S.; Grandinetti, F. *Eur. J. Inorg. Chem.* **2004**, 1125–1130.
- (48) *CRC Handbook of Chemistry and Physics*; CRC Press: Boca Raton, FL, 1985–1986.
- (49) Schröder, D.; Hrušák, J.; Tornieporth-Oetting, I. C.; Klapötke, T. M.; Schwarz, H. *Angew. Chem., Int. Ed.* **1994**, *33*, 212–214.